## SUPPLEMENTAL INFORMATION

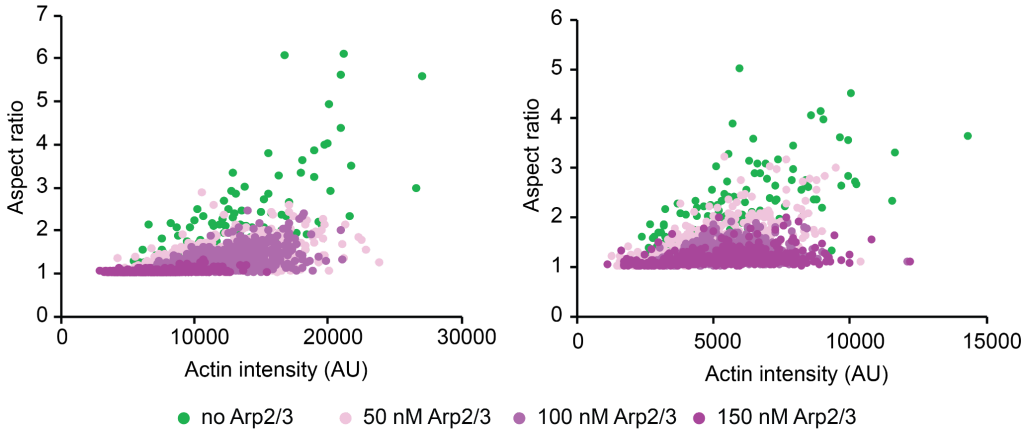


**Supplemental Figure S1. Replicates of figure 3a**. Relationship between droplet aspect ratio and actin intensity within the droplet for droplets formed from 15 μM VASP and exposed to 2 μM actin with increasing concentrations of Arp2/3 and VCA, as visualized in Figure 3a. *Left:* n = 3387 droplets. *Right:* n= 2761 droplets.

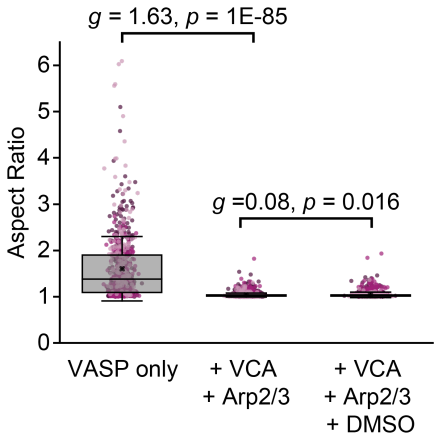


**Supplemental Figure S2. CK666 vehicle DMSO does not impact droplet aspect ratio distribution.** DMSO was added to 15 μM VASP droplets composed of 150 nM Arp2/3, 6 μM VCA, and 2 μM actin. The final concentration was 2% DMSO to match the concentration used in the CK666 experiment in figure 3e. Brackets show data tested for effect size using Hedges g, and significance using an unpaired two tailed t-test.

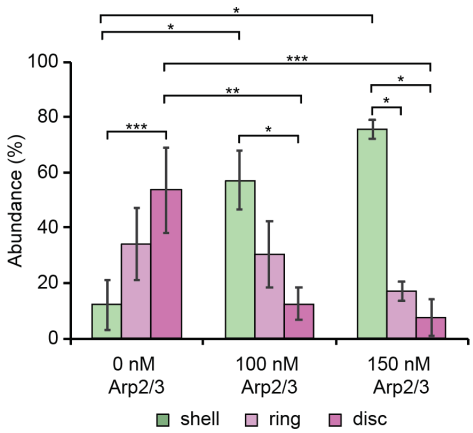


**Supplemental Figure S3. Statistical tests for Figure 4f.** Any comparisons between groups not designated with an asterisk are not statistically significant ($p>0.05$). Asterisks show data that was tested for significance using an unpaired, two-tailed t-test. * denotes $p < 0.05$, ** denotes $p < 0.01$, *** denotes $p < 0.001$. n=3 biologically independent replicates.

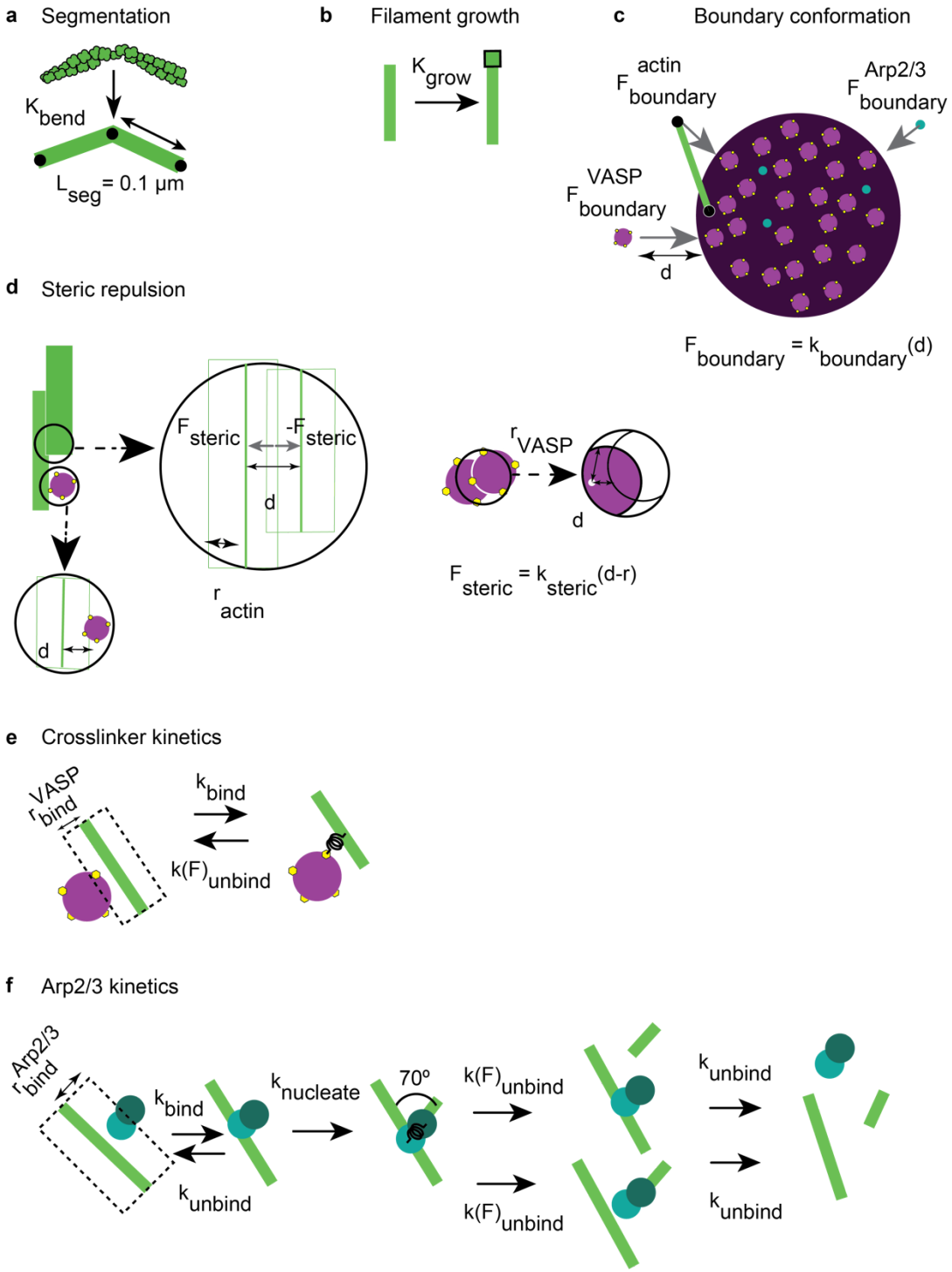


**Supplemental Figure S4. Depictions of model parameters.** (a) Actin filament curvature is approximated through a series of line segments of length $L_{seg}$. (b) Propensity of filament growth is calculated from the product of the G-actin monomers available in the volume and the filament growth rate $K_{grow}$. (c) Actin (green), VASP tetramers (purple spheres), and Arp2/3 (teal) molecules are constrained within the droplet volume through harmonic potentials. (d) Steric repulsion potentials prevent spatial overlap of molecules within the droplet. (e) VASP binding sites (shown as yellow hexagons) located within the binding distance $r_{bind}^{VASP}$ stochastically bind actin filaments at rate $k_{bind}$. Force sensitive unbinding reaction is also included. (f) Diffusing Arp2/3 molecules within binding distance $r_{bind}^{Arp2/3}$ bind actin

stochastically at rate $k_{bind}$. Branched nucleation at rate $k_{nucleate}$ results in an offspring filament at 70º angle with the parent filament. Force-sensitive unbinding reactions at rate kunbind are also considered. Please refer to Supplementary Table S1 for a detailed table of various parameters used in the model.

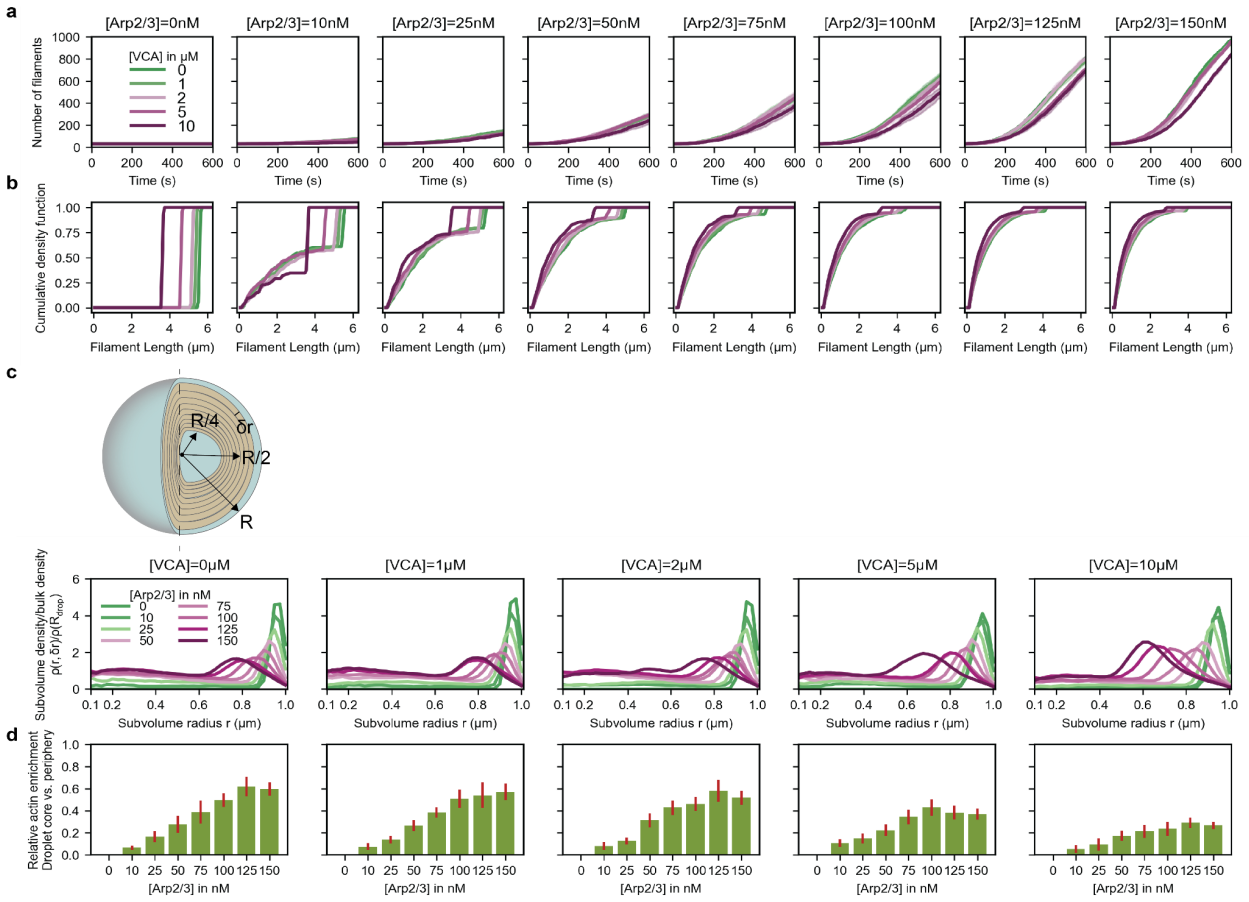


**Supplemental Figure S5. VCA reduces nucleation rate, filament length, and reduces actin enrichment at the core.** (a) Mean (solid line) and standard deviation (shaded area) in the number of actin filaments are plotted as time traces and colored based on the concentration of VCA. (b) The final distribution of filament lengths (last 10 snapshots per replicate) is plotted as a cumulative density function and colored by VCA concentration. Data from 3 replicates. (c) Each subpanel shows the mean ratio of actin density within subvolume shells of radius r and thickness $\delta r = 25\,nm$ to the overall density of actin within the droplet of radius R at a given VCA concentration (mentioned above). Plot lines are colored based on Arp2/3 concentration. Diagram depicts subvolume shells, with shells of radius r = R/4, R/2, and R highlighted, with $0 \leq r \leq R$. (d) Actin enrichment close to droplet core is calculated at various [Arp2/3] as the ratio of the maximum actin density in the core and periphery. As actin peaks are found close to $r = 0.5\mu m$ in some cases ([VCA]=10 $\mu M$, last column), we define core as $0.2 \leq r_c < 0.4$ and periphery as $r_p \geq 0.4$. Data from 3 replicates, the last 10 snapshots per replicate were used here.

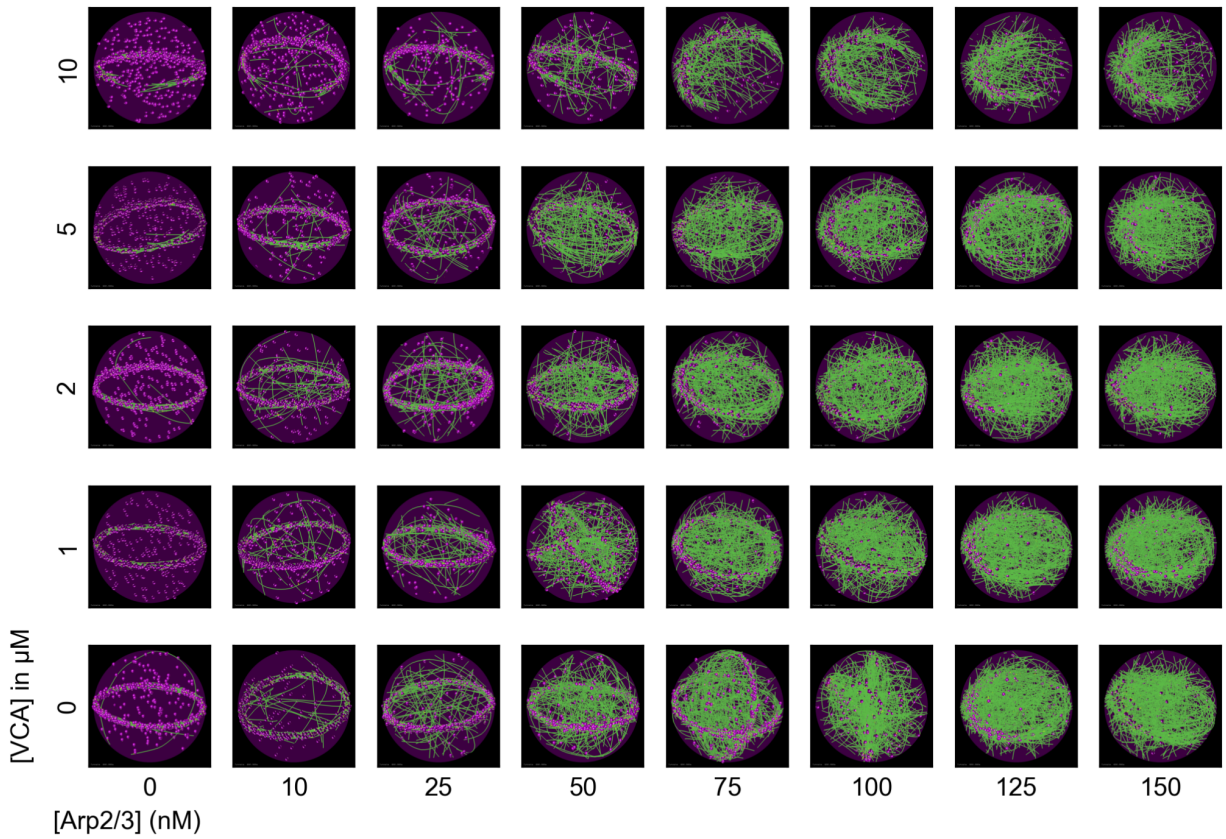


**Supplemental Figure S6. VCA competes for actin and alters spatial distribution of actin but not overall network shape.** Representative final snapshots (t=600s) from rigid droplets (radius = 1 µm) [VASP-tet] = 0.2 µM at various Arp2/3 and VCA concentrations are shown. Actin filaments are shown in green while VASP tetramers are shown as magenta spheres. VCA is not explicitly represented in this model. The effect of VCA is accounted for by modeling VCA as a species that competes for total actin. Please refer to Supplementary Methods for a detailed description of the VCA model. We see that up to [Arp2/3]=25nM, increasing VCA causes partially-formed rings. At higher [Arp2/3] concentrations, we see marked increase in actin concentration closer to the droplet core at all [VCA] studied. Analyzing filament characteristics, we see that median filament length is reduced as [VCA] is increased which also diminishes the autocatalytic Arp2/3-driven nucleation (Supplementary Figure S5a-b). Particularly, the length reduction is weaker than that from the increase in Arp2/3. Calculations of local versus bulk density and relative actin enrichment (Supplementary Figure S5 c-d), show enhanced actin enrichment at the core at any given [VCA]. Additionally, the extent of accumulation at a given [Arp2/3] diminishes with increasing [VCA]. Thus Arp2/3-driven nucleation has a stronger impact on actin organization than VCA in the conditions studied.

**Table S1.** Table of parameters used to set up the actin model in Cytosim.

| **Parameter** | **Value** | **Notes/Reference** |
|---|---|---|
| Total time | 600 s | Experimental images are taken at 600s |
| Implicit evolution time step | 0.001 s | |
| Viscosity of droplet medium | 0.5 pN.s/$\mu m^2$ | 50x water |
| **Boundary** | | |
| Shape | Sphere | |
| Radius | 1 μm | |
| Boundary repulsion stiffness | 200 pN/μm for actin filaments and 100pN/μm for VASP | This spring stiffness acts on points if they move outside the boundary and the force depends on the distance outside the boundary. Here the stiffness depends on the distance outside the boundary<br>Figure S4c |
| **Actin filaments** | | |
| Segmentation length, $L_{seg}$ | 100 nm | Figure S4 |
| Maximum length | $2\pi R_{drop}$ μm | $R_{drop}$ is radius of droplet |
| Growth rate $k_{grow}$ | 0.0103μm/s | Please refer to Supplementary Methods for details on the filament growth model<br>Figure S4b |
| Brownian ratchet force for polymerization | 10 pN | (1) |
| Actin flexural rigidity $K_{bend}$ | 0.075 pN.$\mu m^2$ | (2) |
| Actin steric repulsion $K_{steric}^{Actin}$ | Radius 3.5 nm<br>Stiffness 1.0 pN/μm | (3) |
| **VASP tetramers** | Figure S4E | |
| Radius | 30 nm | |
| Diffusion rate | 10 $\mu m^2$/s | |

| | | |
|---|---|---|
| Concentration of tetramers [VASP-tet] | 0.4μM (1000 molecules of VASP-tetramer) | |
| Binding rate $k_{bind}^{VASP}$ | 1.0 (1/s) | (3) |
| Binding distance | 30 nm | This distance represents the proximity between an actin filament and a VASP molecule required to ensure binding. This value was chosen after a parameter sweep to ensure adequate crosslinking is observed in the simulations. |
| Valency | 4 | Each spherical molecule approximates a tetrameric VASP |
| Unbinding rates $k_{unbind}^{VASP}$ | 1.0 (1/s) | (3) |
| Characteristic unbinding force | 10 pN | Typical values for passive crosslinkers |
| VASP steric repulsion $K_{steric}^{VASP}$ | Radius 30 nm<br>Stiffness 1.0 pN/μm | Chosen to ensure ring formation is observed in the kinetic parameters explored in Figure 4 |
| **Arp2/3** | Figure S4F | |
| Arp2/3 concentration [Arp2/3] | {0, 10, 25, 50, 75, 100, 125, 150} nM<br>{0, 25, 63, 126, 189, 252, 315, 378 } molecules | Varied in this study |
| Binding rate $k_{bind}^{Arp}$ | 0.5/s | determined empirically. $k_{bind}^{Arp}$=0.5/s exhibited 10x increase in the initial number of filaments when [Arp2/3]=50 nM. |
| Unbinding rate $k_{unbind}^{Arp}$ | 0.005 /s | (4) |
| binding distance | 12nm~4.72nm+7nm | Arp2/3 radius = 4.72 nm (5)<br>Actin diameter = 7 nm (6) |
| Nucleation rate $k_{nucleate}$ | 0.2/s | (7) |
| branching angle | $70^{\circ}$ | (8) |
| angle stiffness to ensure branching angle | 0.076 pN.μm/rad | (9) |
| Arp2/3-parent filament and Arp2/3-offspring | 6pN | (10) |

| | | |
|---|---|---|
| filament unbinding force | | |

## SUPPLEMENTAL MOVIES

**Supplemental Movie M1.** VASP droplets formed with Arp2/3 and VCA still undergo fusion.
**Supplemental Movie M2.** VASP droplets formed with Arp2/3 and VCA still exhibit fast and complete recovery after photobleaching.
**Supplemental Movie M3.** Simulation time-lapse of droplets with increasing Arp2/3 results in less bundled rings and more central actin accumulation.
**Supplemental Movie M4.** Simulation time-lapse of droplets with increasing VCA at various Arp2/3 concentrations shows VCA competes for actin to alter spatial distribution of actin.

## SUPPLEMENTAL METHODS

### Chemical and mechanical framework employed in CytoSim

Cytosim (https://gitlab.com/f-nedelec/cytosim) is an agent-based framework to simulate cytoskeletal networks with physical realism subject to geometric constraints. In Cytosim, each time step (1ms in this study) involves the evolution of chemical reactions based on their propensities, followed by Brownian dynamics evolution of the chemical species to capture diffusion effects. Filament extension is modeled as follows: Assuming a growth rate of 0.0103 μm/s, we solved the following ordinary differential equations in series to identify the total actin parameter to use in Cytosim [T-Actin].

| Symbol | Represents concentration of |
|---|---|
| [P] | Plus End |
| [G-actin] | unpolymerized actin |
| [F-actin] | Polymerized actin |
| $N_{fil}$ | Number of filaments |

$$[T-actin] = [G-actin] + [F-actin] \quad (1)$$

$$\frac{d[F-actin]}{dt} = k_{grow} N_{fil}\left(1 - \frac{[F-actin]}{[T-actin]}\right) \quad (2)$$

These equations were solved with initial conditions $t = 0,\ N_{fil} = 30,\ [F-actin](0) = 0.44\ \mu M$ along with boundary conditions $t = 600s,\ [F-actin](600) = 27.68\ \mu M$. The number of actin monomers corresponding to t=600s can be calculated to be 69,823 molecules.The boundary condition corresponds to per actin filament length of $2\pi\ \mu m$. Solving this numerically in Python using scipy.integrate, we find that [T-actin]=138.38 $\mu M$. Please note that while this value is significantly higher than the concentration of actin used in experiments, the value is just one of many degenerate ($k_{grow}$, [T-actin]) value pairs that would numerically satisfy the equations (1) and (2).

To capture essential chemical reactions observed in VASP droplets, filament extension is modeled as a deterministic force-sensitive process as described above along with stochastic Monte Carlo sampling of crosslinker binding and its force-sensitive unbinding reactions. Arp2/3 binding, nucleation, and unbinding are all modeled as stochastic reactions.

### Representation of actin filaments

Actin filaments are represented as inextensible fibers represented as a series of linear segments. The upper limit of segment length is 100 nm. CytoSim computes bending energy of the fiber based on the flexural rigidity specified in the input parameters.

**Representation of VASP tetramer**

We model VASP as a spherical crosslinker of radius 30 nm with four F-actin binding sites distributed across the surface of the sphere. Cytosim also requires specification of a binding distance parameter between VASP and actin. As we are interested in the changes to ring-shaped actin networks, we used the parameters from our previous study (3) that resulted in the formation of ring-shaped networks.

**Representation of Arp2/3**

Arp2/3 molecules are modeled as diffusing point particles. The binding, nucleation, and unbinding reactions are considered as shown in Supplemental figure S4f. In our simulations, Arp2/3 nucleation produces filaments of 5 nm in length at a 70$^{o}$ angle with respect to the parent filament.This offspring filament then extends through actin polymerization.

**Position evolution**

The diffusion of VASP, points along the actin filaments and Arp2/3 molecules are considered in Cytosim through a Langevin equation framework. For a particle i, the coordinates are given by xi = {xi1, xi2, xi3}. The position along each of the dimensions j is evolved according to the stochastic differential equation given by,

$$dx^{ij}(t) = \mu f^{ij}_{tot}(t)\, dt + dB_j(t)$$

Here, μ is the viscosity of solvent, and $f^{ij}_{tot}(t)$ represents the total force acting on the particle at time t. The diffusion term (noise) is given by a random variable sampled from a distribution with mean 0 and standard deviation $\sqrt{2D^i dt}$, where the diffusion coefficient is given by $D^i = \mu k_B T$ where T is temperature and $k_B$ is Boltzmann constant. Please refer to Supplementary Table S1 for a detailed description of parameters used in this study.

**Analysis of trajectories**

Five trajectories were generated for each [Arp2/3] concentration studied. We wanted to understand the distribution of actin within the droplet. Toward this, we discretized the droplet into subvolume shells of varying radii of a finite thickness (δ=25 nm). We calculated the ratio of the local density within shells and the bulk density as,

$$\frac{\rho(r,\delta r)}{\rho(R_{drop})} = \frac{N(r,\delta r)/r^2 \delta r}{N_{total}/R^3}$$

Here, N total refers to the total number of actin monomers in the system. $N(r, \delta r)$ represents the number of actin monomers in shell of radius r and thickness $\delta r$.

Further, we also calculated the relative actin enrichment (R.A.E) in the core with respect to the periphery of the droplet as follows. We define the actin core to be $r_c \in [0.2, 0.6]\mu m$ and periphery to be $r_p > 0.6\mu m$. The subvolume (of thickness 25nm) with maximum density in the core ($\rho(c, \delta r) = max\{\rho(r_c, \delta r), r_c \in [0.2, 0.6]\}$) and periphery ($\rho(p, \delta r) = max\{\rho(r_p, \delta r), r_p \in (0.6, 1.0)\}$) are identified.

The relative actin enrichment (R.A.E.) is defined as,

$$R.A.E. = \frac{\rho(c,\delta r)}{\rho(p,\delta r)}$$

**Modeling role of VCA**

In addition to binding and activating Arp2/3, VCA is also known to bind G-actin. We assume that all Arp2/3 molecules in our simulations are constitutionally active. To account for the G-actin competition by VCA, we followed the following protocol in CytoSim. Under this framework, VCA is not explicitly represented but rather accounted for passively as a chemical species that competes for actin. To achieve this phenomenology, we model VCA using the fibers module. VCA is modeled as a single fiber that is mechanically inert with respect to actin and VASP. VCA fiber competes for total available actin according to the following equation.

$$\frac{d[VCA-actin]}{dt} = k_{bind} N_{VCA}(1 - \delta) = k^{fiber}_{bind}\ (1 - \delta) \qquad (3)$$

$$\delta = \begin{cases} \frac{[F-actin]+[VCA-actin]}{[T-actin]}, \text{ when } [VCA - actin] < [G_{max}] \\ 1, \text{ otherwise} \end{cases}$$

Where $N_{VCA}$ represents the number of VCA molecules considered. $k^{fiber}_{bind} = k_{bind} N_{VCA}$ is the growth rate that is used in CytoSim input files. $[G_{max}]$ represents the maximum concentration of actin that is no longer available for polymerization. $[G_{max}]$ and $k_{bind}$ were empirically chosen using an ODE model solving Eqs. (1)-(3) such that $[VCA] = 1\mu M$ reduces $[F - actin]$ at t=600s by $1\mu M$. In this study, we use $k_{bind} = 3.44\mu m/s$, $[G_{max}] = 5 \times [VCA]$.

Here, we provide a sample calculation for the parameters that were used in the CytoSim input file. For example, for a spherical reaction volume of radius $1\mu m$, $[VCA] = 1\mu M \Rightarrow N_{VCA}$ =2522 molecules.

$k^{fiber}_{bind} = k_{bind} N_{VCA} = 8675.68\mu m/s$ Assuming each actin increases filament length by 2.7nm, $L_{Gmax} = [G_{max}] = 0.0027 \times 5 \times N_{VCA} = 34.047\ \mu m$.

```
set fiber vca
{
    rigidity = 0.00001
    segmentation = 0.1
    confine = inside, 200, cell
    display = ( line=5, 0; color=0x5CBA47FF; )
    activity =grow
    growing_speed = 8675.68, 0
    growing_off_speed = 0, 0
    growing_force = inf
    total_polymer = 942.4777960769379
```

```
    max_length = 34.047000000000004
    min_length = 0.0027
    steric = 0
    binding_key = 2
}

new 1 vca
{
    length = 0.1
    end_state = 1, 0
}
```

As CytoSim does not permit competition for actin between two filament types in its default version, the following code edit was also implemented in fiber_set.cc. The specific lines that were added are highlighted in bold.

```
void FiberSet::step()
{
PropertyList plist = simul.properties.find_all("fiber");
// calculate the total length used for each kind of Fiber:
for ( Property * i : plist )
static_cast<FiberProp*>(i)->used_polymer = 0;
for ( Fiber const* fib = first(); fib; fib = fib->next() )
fib->prop->used_polymer += fib->length();
// Get total used polymer
auto total_used_polymer = 0.0;
for ( Property * i : plist )
total_used_polymer = total_used_polymer +
                        static_cast<FiberProp*>(i)->used_polymer;
// set the total to be sum of all fiber types
for ( Property * i : plist ){
      static_cast<FiberProp*>(i)->used_polymer = total_used_polymer;
// calculate the ratio of free polymer for each class of Fiber:
for ( Property * i : plist )
{
FiberProp * fp = static_cast<FiberProp*>(i);
// update the normalized monomer concentration:
fp->free_polymer = 1.0 - fp->used_polymer / fp->total_polymer;
if ( fp->free_polymer < 0 )
{
Cytosim::warn << "The free monomer concentration would be negative !!!\n";
//this should not happen
fp->free_polymer = 0;
}
}
```

## REFERENCES


1. A. Mogilner, G. Oster, Cell motility driven by actin polymerization. *Biophys J* **71**, 3030–3045 (1996).
2. F. Gittes, B. Mickey, J. Nettleton, J. Howard, Flexural rigidity of microtubules and actin filaments measured from thermal fluctuations in shape. *Journal of Cell Biology* **120**, 923–934 (1993).
3. A. Chandrasekaran, K. Graham, J. Stachowiak, P. Rangamani, Kinetic trapping organizes actin filaments within liquid-like protein droplets. 2023.05.26.542517 (2023).
4. N. G. Pandit, *et al.*, Force and phosphate release from Arp2/3 complex promote dissociation of actin filament branches. *Proceedings of the National Academy of Sciences* **117**, 13519–13528 (2020).
5. M. Boczkowska, *et al.*, X-Ray Scattering Study of Activated Arp2/3 Complex with Bound Actin-WCA. *Structure* **16**, 695–704 (2008).
6. E. H. Egelman, The structure of F-actin. *J Muscle Res Cell Motil* **6**, 129–151 (1985).
7. B. A. Smith, K. Daugherty-Clarke, B. L. Goode, J. Gelles, Pathway of actin filament branch formation by Arp2/3 complex revealed by single-molecule imaging. *Proceedings of the National Academy of Sciences* **110**, 1285–1290 (2013).
8. R. D. Mullins, J. A. Heuser, T. D. Pollard, The interaction of Arp2/3 complex with actin: Nucleation, high affinity pointed end capping, and formation of branching networks of filaments. *Proceedings of the National Academy of Sciences* **95**, 6181–6186 (1998).
9. M. Akamatsu, *et al.*, Principles of self-organization and load adaptation by the actin cytoskeleton during clathrin-mediated endocytosis. *eLife* **9**, e49840 (2020).
10. I. Fujiwara, S. Suetsugu, S. Uemura, T. Takenawa, S. Ishiwata, Visualization and force measurement of branching by Arp2/3 complex and N-WASP in actin filament. *Biochemical and Biophysical Research Communications* **293**, 1550–1555 (2002).